



cambridge.org/mrf

Ahmed Z. A. Zaki¹ , Ehab K. I. Hamad² , Tamer Gaber Abouelnaga^{3,4}
and Hala A. Elsadek³

Research Paper

Cite this article: Zaki AZA, Hamad EKl, Abouelnaga TG, Elsadek HA (2022). Design of ultra-compact ISM band implantable patch antenna for bio-medical applications. *International Journal of Microwave and Wireless Technologies* **14**, 1279–1288. <https://doi.org/10.1017/S1759078721001732>

Received: 13 July 2021
Revised: 1 December 2021
Accepted: 8 December 2021
First published online: 6 January 2022

Keywords:

Antenna for biomedical applications; implanted antenna; medical implant communication service band (MICS); medical monitoring

Author for correspondence:

Ahmed Z. A. Zaki,
E-mail: azakaria64@gmail.com

¹Communication Department, Modern Academy for Engineering and Technology, Cairo, Egypt; ²Electrical Engineering Department, Faculty of Engineering, Aswan University, Aswan 81542, Egypt; ³Microstrip Circuits Department, Electronics Research Institute, Cairo, Egypt and ⁴Higher Institute of Engineering and Technology, Kafr El-Shiekh, Egypt

Abstract

In this paper, an ultra-compact implantable antenna for biomedical applications is proposed. The proposed implanted meandered compact patch antenna is implanted inside the body at a depth of 2 mm. The proposed antenna was designed with Roger RO3003 ($\epsilon_r = 3$) as substrate with an overall size of dimensions $5 \times 5 \times 0.26 \text{ mm}^3$. The radiating element is a square patch antenna with different size rectangular slots and coaxial feeding. The proposed implantable antenna resonates at 2.45 GHz (from 2.26 to 2.72 GHz) frequency with a bandwidth of 460 MHz and a gain of -22.6 dB . The specific absorption rate has been considered for health care considerations, and the result is within the limits of the federal communication commission. The measured and simulated scattering parameters are compared, and good agreements are achieved. The proposed antenna is simulated and investigated for biomedical applications suitability.

Introduction

In recent days, as a result of the development of medical applications technology, wireless implanted devices (biomedical devices) have significant attention. Day after day, the demand for implanted medical devices (IMD) increases, as more than 3 million people around the world have these devices such as pacemakers [1]. The need for IMD is increasing to improve the lifestyle of a chronic disease patient. The patient will not have to visit the doctor because he can monitor the patient's vital functions in real-time, even when the patient is at home [2]. There are many applications for IMDs, such as cancer treatment using hyperthermia [3] and injecting the patient with his appropriate dose of drug remotely and monitoring his vital signs [4].

In order for implanted devices to monitor the vital functions of the human body, such as blood pressure, temperature, etc., the devices need to be placed inside the human body to send the data to outer devices (base station), which is engaged with the patient to receive the information from IMD then take the proper action [5, 6] (Fig. 1).

There are many applications of IMD as monitor health caring that include pacemakers [7], cochlear and retinal implants [8, 9], glucose sensors [10], diagnosis of the hypopnea syndrome [11], and chronic obstructive pulmonary disease warning [12–14].

The IMD must support at least one of those frequency bands according to standard regulation [15–17]: 402.0–405.0, 420.0–450.0, 863.0–870.0, 902.0–928.0, 950.0–958.0, 2360.0–2400.0, and 2400.0–2483.5 MHz and WMTS bands (608–614 MHz, 1.395–1.400 GHz) and also ultra-wide band (UWB) IMDs, which implement low band (3494.4–4492.8 MHz) or high band (6489.6–9984.0 MHz) [18].

Therefore, designing implantable antennas has been received significant attention from scientific researchers nowadays for its wide usage in many medical applications. Some requirements must be taken into account when designing, such as patient safety, biocompatibility, miniaturization, and quality of communication with outer devices [19]. Patch antenna receives major attention in implantable applications because its design is flexible and compatible with most applications [20, 21]. It allows for reducing antenna size easily and integrates it in the IMD [22].

This work proposes a new miniaturized implantable antenna for biomedical applications resonating over the Industrial, Scientific, and Medical (ISM) band of 2.26–2.72 GHz. This paper is organized as follows: section “Antenna design and simulation” presents the proposed implantable antenna configuration and its simulation results. Section “Measurements” discusses the experimental results and their analysis. Finally, the conclusion is presented in section “Conclusions”.

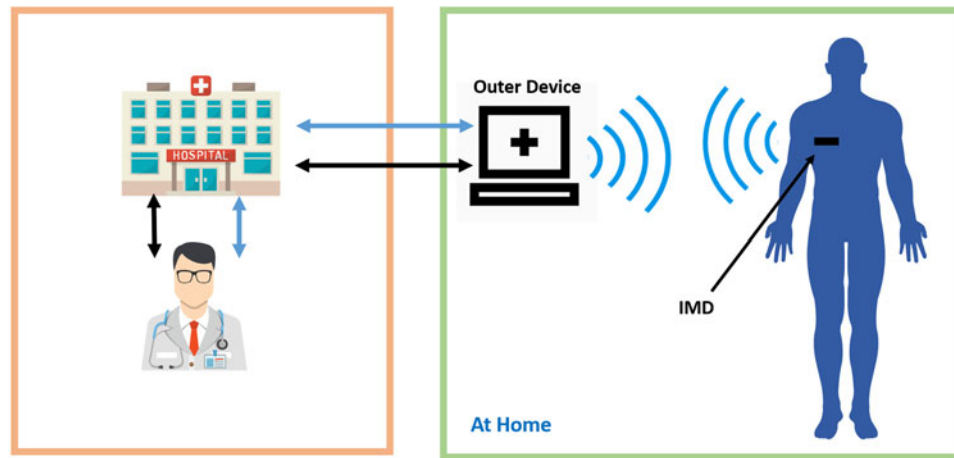


Fig. 1. Health care monitoring using IMDs.

Antenna design and simulation

Background

The compact size antennas have attracted the attention of many researchers due to their use in many essential applications [23]. Many miniaturization techniques are used recently, such as periodic structure [24], split-ring resonator [25], high-permittivity dielectric (substrate/superstrate) [19], increase current path length, and use short pins [26].

By comparing the antennas in the free space and those implanted inside the human body, the radiation characteristics have been found, such as gain of the implanted antenna is below zero because of losses happened due to surrounding human tissues. The human body is made of different layers (skin, fat, and muscle), with nonlinear electrical characteristics. The dielectric constant (ϵ_r) and conductivity (σ) of these layers of the human body at 2.45 GHz are listed in Table 1 [22].

Table 1. The dielectric properties of different layers of the human body at 2.45 GHz [22]

Tissue type	Dielectric constant (ϵ_r)	Conductivity (σ s/m)
Skin	38	1.44
Fat	5.28	0.1
Muscle	52.7	1.74

Another constraint parameter that defines the amount of allowed power incident on the human body is the specific absorption rate (SAR) [27]. The IEEE standard allowed the average SAR for a 1 g of cube-shaped tissue to be <1.6 W/kg, while the ICNIRP (International Commission on Non-Ionizing Radiation Protection) basic restrictions limit the SAR averaged over 10 g of contiguous tissue to <2 W/kg [27, 28].

Antenna configurations

The implanted antenna should be as small as possible because the allowed space is limited to implant it easily inside the patient body. So, the implanted meandered compact patch (IMCP) antenna was designed on 0.13 mm-thick Roger RO3003 ($\epsilon_r = 3$) as a substrate material to operate at the ISM band 2.4 GHz with an overall volume of $5 \times 5 \times 0.26$ mm³ as illustrated in Fig. 2. The Optimized dimensions of the proposed IMCP antenna are tabulated in Table 2. The patch is covered with the same material of 0.13 mm superstrate to prevent short circuits and at the same time to reduce the parasitic coupling of electromagnetics with human tissues and to help in miniaturizing the antenna size by reducing the operating frequency to the lower side of the spectrum [19].

To maintain patient safety and prevent the short circuit, the antenna is covered with a biocompatible material. The antenna is covered with a thin layer of ceramic alumina (Al_2O_3) with a permittivity of 9.8 and 0.008 loss tangent with a thickness of 0.02 mm to protect the designed antenna.

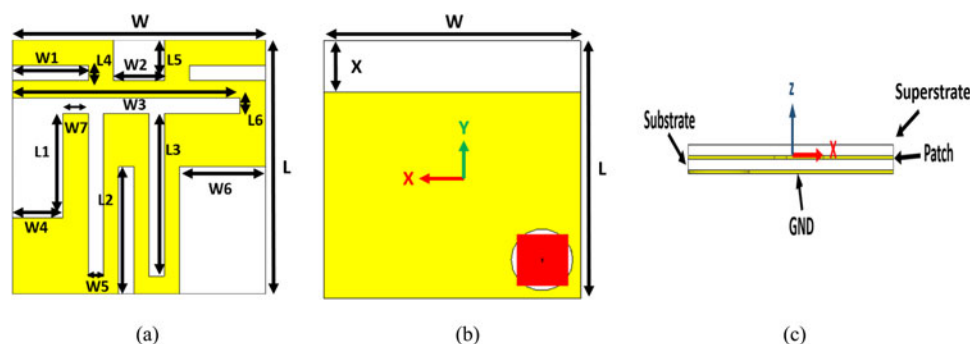


Fig. 2. The geometry of the IMCP proposed antenna, (a) patch, (b) ground, (c) side view.

Table 2. Optimized dimensions of the proposed IMCP antenna

Parameters	Values (mm)	Parameters	Values (mm)
L	5	W	5
L_1	2	W_1	1.5
L_2	2.5	W_2	1
L_3	3.2	W_3	4.5
L_4	0.3	W_4	1
L_5	0.5	W_5	0.3
L_6	0.3	W_6	1.7
X	1	W_7	0.5

The current path is extended over the surface of the patch by meandering the radiating patch; as a result, the ultra-compact size of the antenna is obtained. To attain the best matching impedance with $50\ \Omega$ coaxial cable, the excitation is placed at $x = 1.75\ \text{mm}$ and $y = 1.75\ \text{mm}$ from the center. Partial ground and various cuts were etched on the conventional square patch and are employed to improve the impedance matching to the $50\ \Omega$ feeding line.

Design steps

The proposed IMCP antenna was miniaturized in four steps, as shown in Fig. 3, and a comparison of the simulated S_{11} of four steps using CST Microwave Studio is demonstrated in Fig. 4.

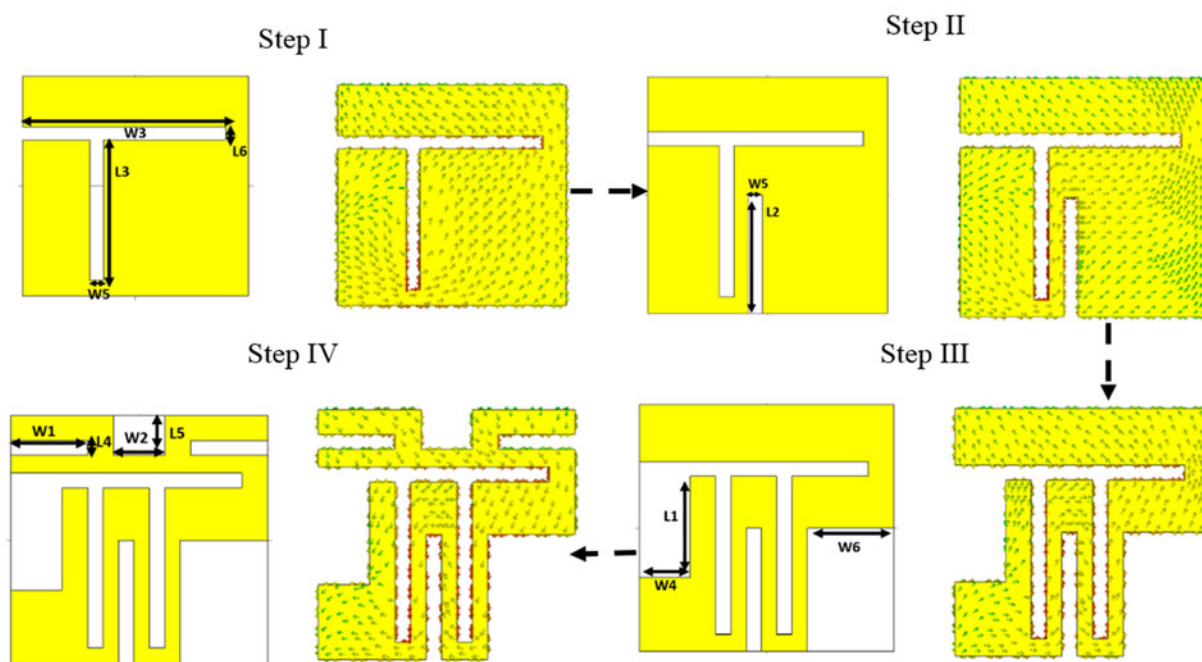


Fig. 3. Miniaturization steps of the proposed IMCP antenna.

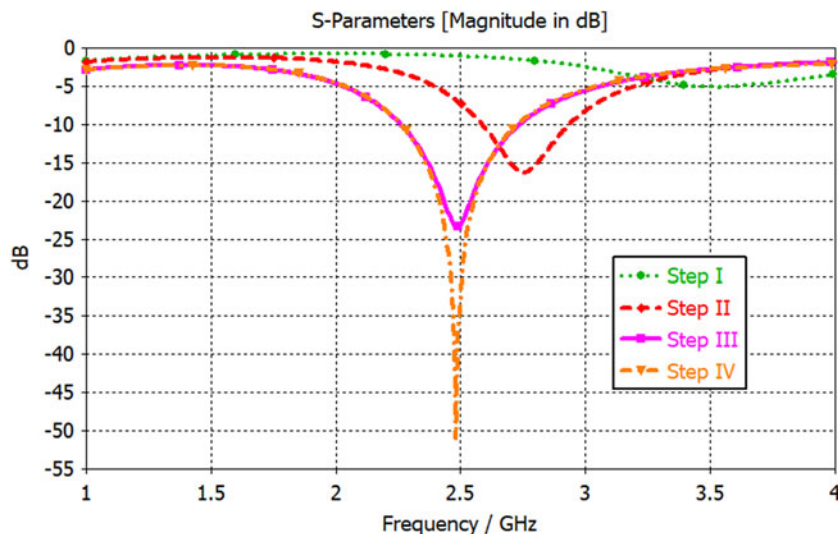


Fig. 4. Comparison of the simulated S_{11} of the miniaturization four steps proposed IMCP antenna using CST Microwave Studio.

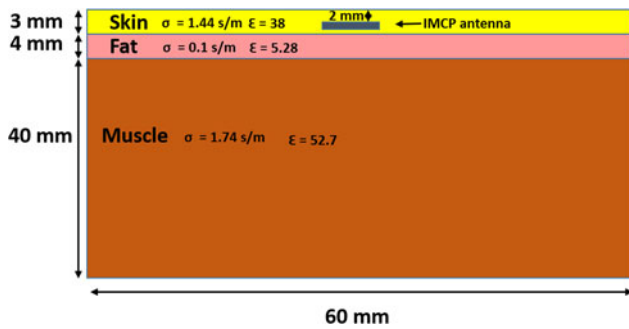


Fig. 5. Three-layer phantom constructed in CST Microwave Studio [22].

Initially, the design was started by using a traditional square patch with two slots of widths W_3 and W_5 . One resonance frequency was obtained at 3.5 GHz, as shown in Fig. 4, step I. Adding more slots to prolong the length of the current path, resulting in the frequency-shifted down to 2.7 GHz as shown in Fig. 4, step II. Adding two more slots are incorporated for more shift down of the resonance frequency to 2.5 GHz as shown in Fig. 4, step III. Adding further slots within the patch, in addition to creating a partial ground in order to improve the antenna gain and enhance the impedance matching up to -50 dB for the S_{11} over a BW of about 420 MHz.

Simulation results

The design and simulations of the proposed IMCP antenna are carried out using CST Microwave Studio 2018 simulator. The

implanted antenna was positioned at a depth of 2 mm from the skin surface, where the human tissue consists of three layers, which are skin, fat, and muscle [22, 28–30]. The simulation model of the human tissue built on CST with the implanted antenna is illustrated in Fig. 5. The thickness of each layer (skin–fat–muscle) is chosen as an average value because the thickness of the layers differs from one person to another and depends on where the antenna is implanted. The electrical properties of the human tissue are mentioned in Table 1.

The simulated reflection coefficient S_{11} , gain, efficiency, and input impedance are illustrated in Fig. 6. As shown in Fig. 6(a), the proposed antenna has a good impedance bandwidth of about 19% (466 MHz) with excellent matching below -10 dB, allowing the antenna to operate properly in the whole ISM band.

The efficiency and gain against the frequency of the proposed antenna were obtained as shown in Figs 6(b) and 6(d). It is clear that the antenna has a peak gain of -22.5 dBi at 2.45 GHz, and it is a good result compared to literature relative to its size of 5×5 mm² and the attenuation due to the surrounding human body.

Input impedance (real and imaginary) is observed as shown in Fig. 6(c); the real part is nearly 48Ω , while the imaginary part is almost 0Ω at resonant frequency; 2.45 GHz. The proposed antenna acts as a good candidate for implantable ISM range applications.

The simulated radiation pattern (E-plane and H-plane) of the IMCP antenna is illustrated in Fig. 7. The antenna is placed in the x - y plane. The proposed antenna has a bi-directional radiation pattern in E-plane with a 3 dB beam width of 60 degrees at 2.45 GHz with a side lobe level of -2.2 dB and a circle radiation pattern in the H-plane.

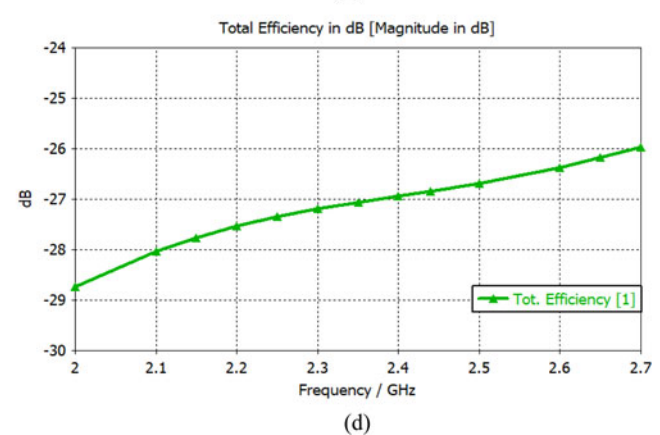
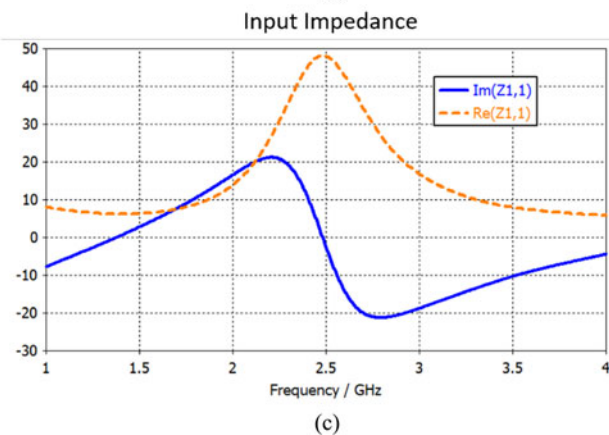
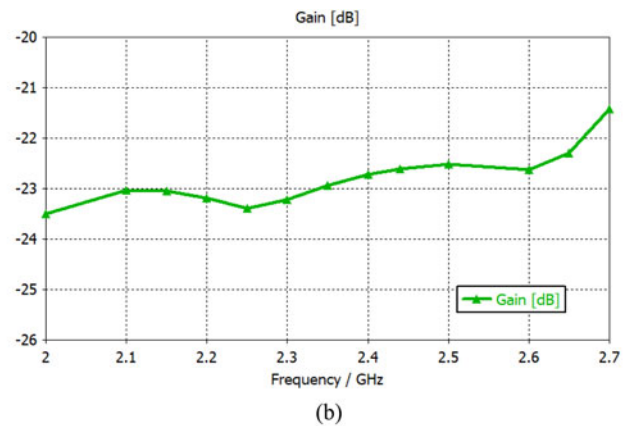
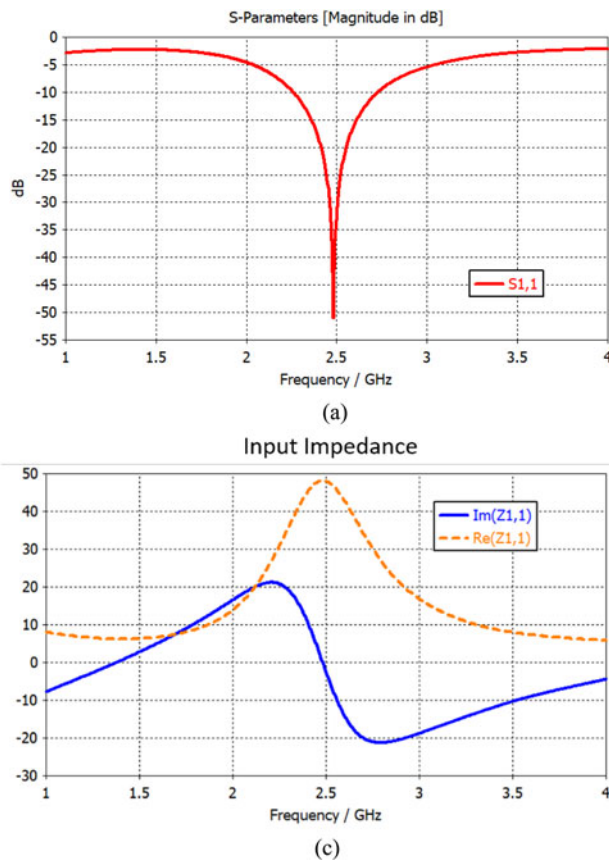


Fig. 6. Simulated (a) S_{11} , (b) gain, (c) Z_{in} , (d) total efficiency of the IMCP proposed antenna.

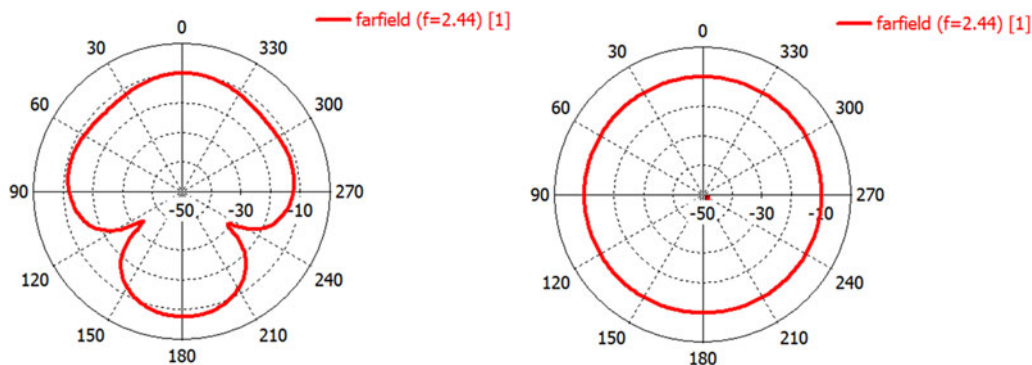


Fig. 7. Radiation patterns of the proposed antenna, E- and H-plane, respectively, at 2.45 GHz.

SAR calculations

To reduce and exclude the harm that can be caused to the human body from exposure to the electromagnetic field due to placing implantable medical devices inside the body, the electromagnetic power should be reduced to a safe value. Because if the body tissue absorbs this electromagnetic power, it could raise the temperature of the tissue, which should not increase more than 1–2 °C [31]. So, various limits are taken to ensure patient safety

At 2.45 GHz, the maximum SAR of the proposed antenna is 40 W/kg over 10 g cubic tissue at an input power of 0.5 W delivered to the antenna. So that, to meet the SAR standard limits, the input power delivered to the proposed antenna must not be increased by more than 24 mW (13.8 dBm) [32–34]. Average SAR distributions at 2.45 GHz over 10 g of human tissue at 500, 24, and 10 mW input power are illustrated in Fig. 8. The SAR is defined by [34]

$$SAR = \sigma|E|^2 / \rho_{den}, \tag{1}$$

where σ is the conductivity of human tissue, E is the intensity of the electric field, and ρ_{den} is the density of human tissue. At present, there is no experimental method for measuring SAR. So, the CST studio as a 3D full-wave simulator has been used to determine the maximum power of the RF radiation to achieve safety standards.

Parametric studies

An intensive parametric analysis of the antenna parameters is carried out to determine the optimum dimensions for the proposed antenna and to explore the parameters that are mainly affecting its performance. It is found that some parameters are affecting the tuning of operating frequency and others affecting antenna matching.

As shown in Figs 9(a) and 9(b), the slot length $L2$ varied from 1.5 to 3 mm, and the slot length $L3$ varied from 0.65 to 2.15 mm. It is observed that as lengths $L2$ and $L3$ increase, the resonant frequency shifted down toward a lower frequency (2.2–2.8 GHz) and

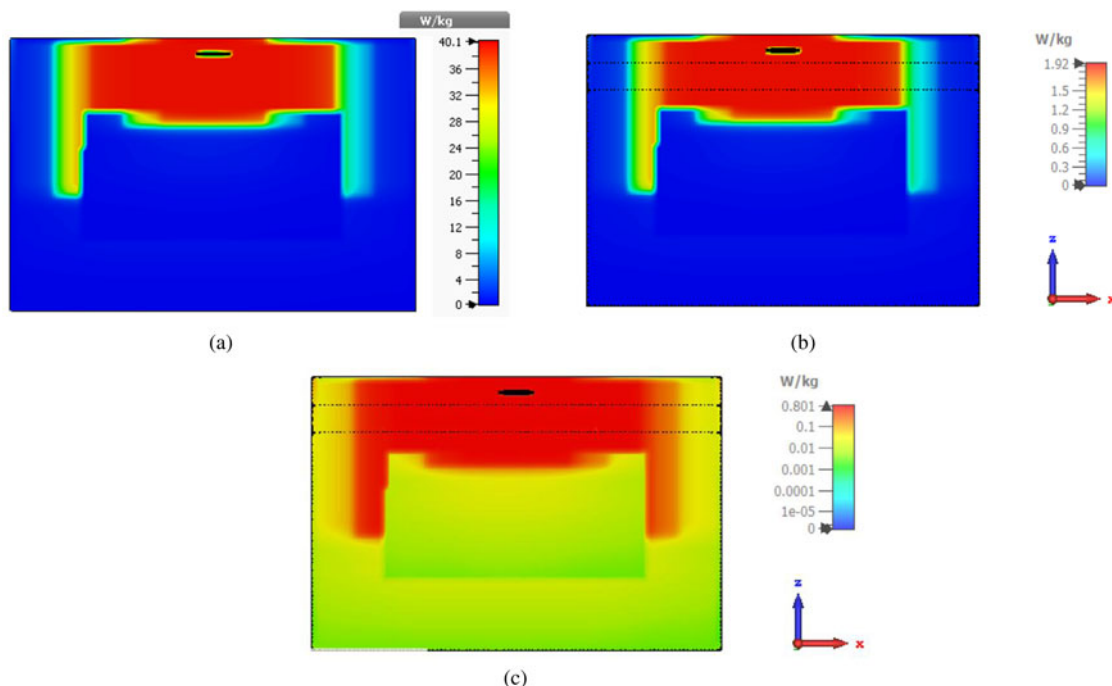


Fig. 8. Average SAR distributions at 2.45 GHz over 10 g of human tissue at (a) 500 mW input power, (b) 24 mW, (c) 10 mW.

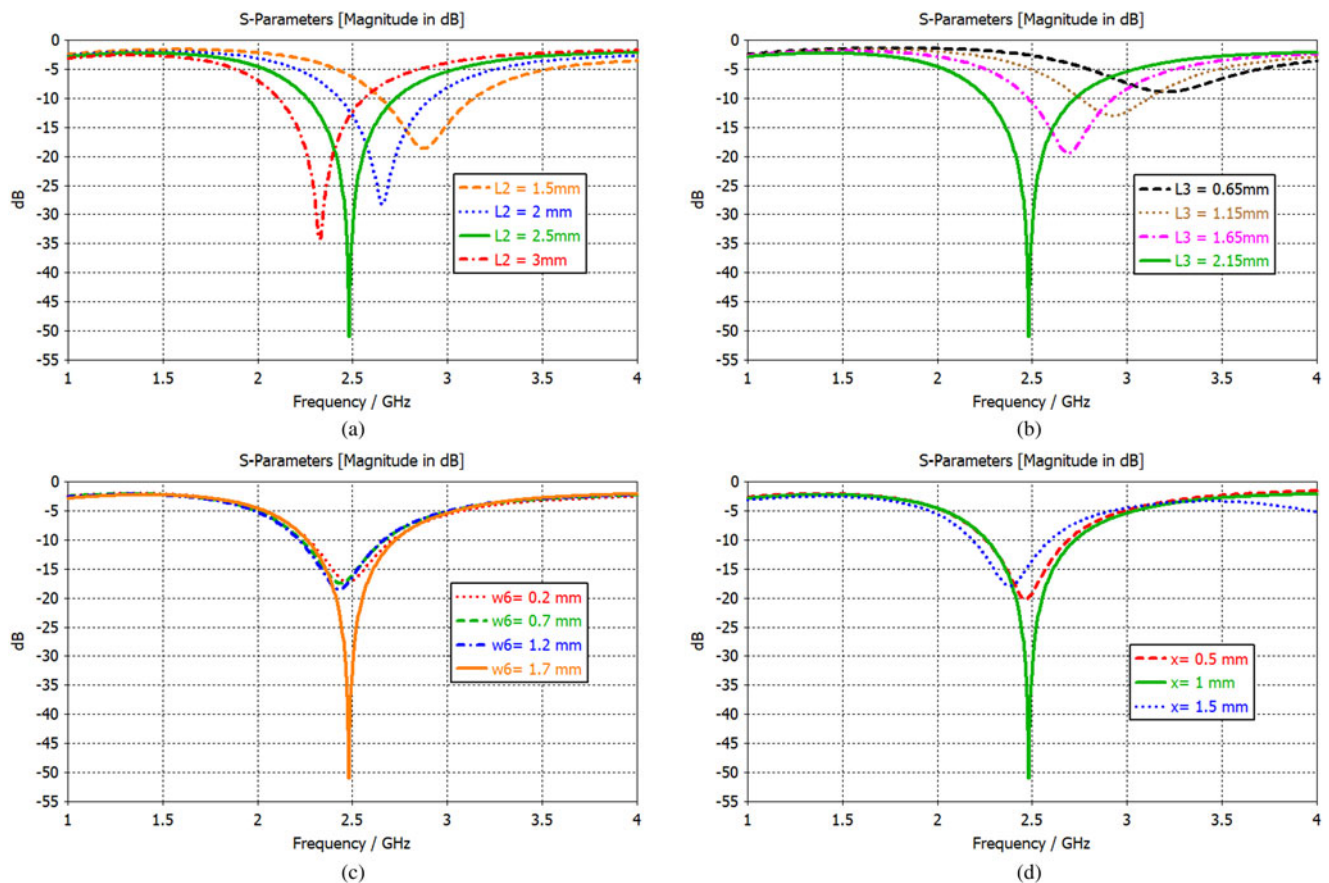


Fig. 9. Effects of variation of (a) L_1 , (b) L_3 , (c) W_6 , and (d) partial ground length.

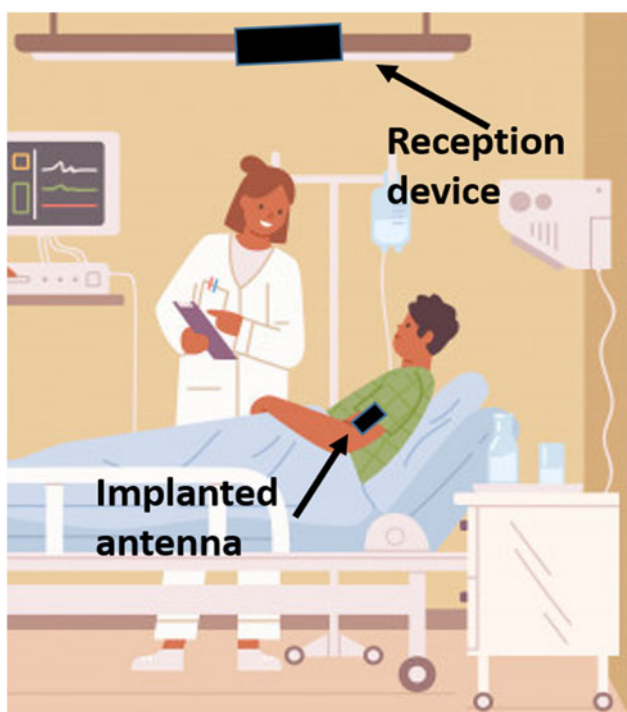


Fig. 10. Proposed patient room.

vice versa. So, we can say that L_2 and L_3 can fully control the resonant frequency.

In Figs 9(c) and 9(d), the width W_6 varied from 0.2 to 1.7 mm, and X varied from 0.5 to 1.5 mm. It is observed that W_6 and X have a significant impact on the antenna matching impedance, and both could be optimized for an acceptable reflection coefficient.

Link budget

Mainly, implanted devices are used to measure physiological signals inside the body and record them using reading devices. Recorded information is transmitted outside the body to the outer device (computer network) through a wireless link, so evaluating the communication link between IMD and the outer receiver should be taken into consideration.

The way to evaluate communication link performance is called link margin (LM) [35]. LM is defined as the difference between actual received power and minimum received signal level. To ensure a good communication link performance, the LM should be >0 dB (+ve value) or equivalently; the LM must be positive. It is calculated as given in [36] as follow:

$$LM \text{ (dB)} = \text{link } C/N_o - \text{required } C/N_o, \quad (2)$$

$$\text{Link } C/N_o = P_t + G_t - L_f - L_a + G_r - 2L_{feed} - N_o, \quad (3)$$

Table 3. LM parameters

Transmission		Receiver		Signal quality	
Frequency [GHz]	2.45	R_x antenna gain G_r [dBi]	2.15	Bit rate B_r [Kb/s]	7/100/1000
T_x power [dB]	-43	PLF [dB]	0	Bit error rate	1×10^{-5}
T_x antenna gain G_t [dBi]	-22.5	Temperature T_0 [K]	293	E_b/N_0 (ideal PSK) [dB]	9.6
		Boltzmann constant K	1.38×10^{-23}	Coding gain G_c [dB]	0
		Noise power density N_0 [dB/Hz]	-200	Fixing deterioration G_d [dB]	2.5

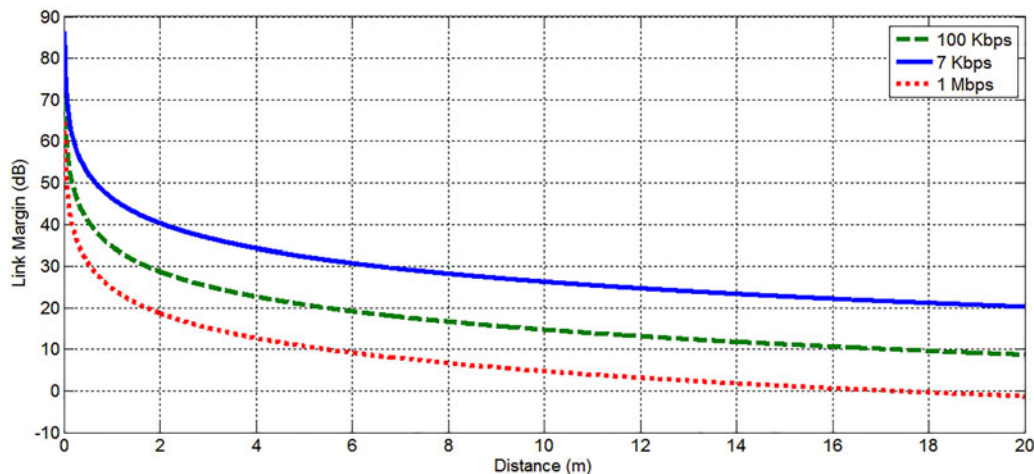


Fig. 11. Calculated link margin at a bitrate of 7, 100 Kbps, and 1 Mbps.

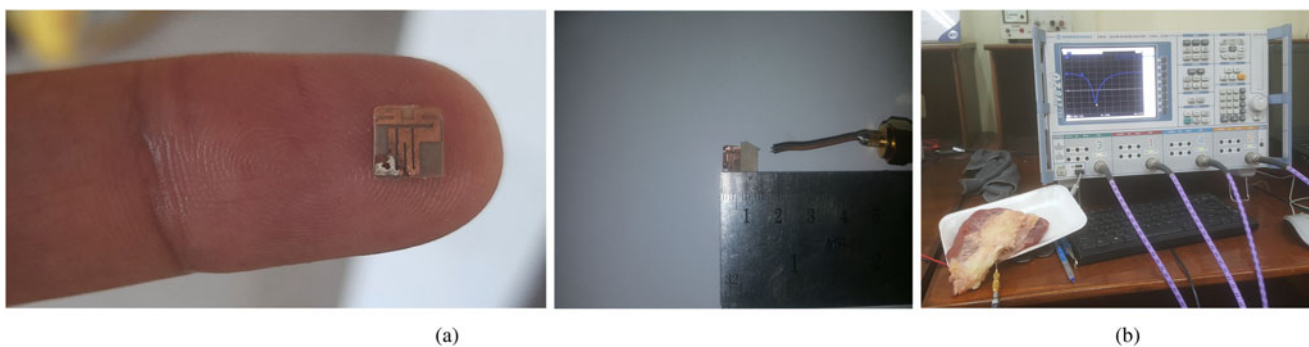


Fig. 12. Photos of the (a) prototypes fabricated antenna and (b) of the measurement setup.

$$\text{Required } C/N_0 = E_b/N_0 + 10 \log (B_r) - G_c + G_d. \quad (4)$$

where P_t is the T_x power, L_{feed} is the feeding loss, G_t is the gain of the transmitter’s antenna, L_f is the free space propagation loss, L_a is the air propagation loss, G_r is the gain of receiver’s antenna, N_0 is the noise power density, E_b/N_0 is the normalized signal-to-noise, B_r is the bit rate, G_c is the coding gain, G_d is the fixing deterioration.

The proposed implanted antenna is assumed to be used in the hospital inpatient room, as demonstrated in Fig. 10. The R_x antenna is assumed to be at about 4–5 m far from the implanted antenna attached to the patient.

The R_x antenna is assumed to be a linear polarized antenna with a gain of about 2.15 dBi, and the T_x antenna is also linearly polarized with a gain of about -22.5 dBi. So, polarization mismatching losses could be neglected for good alignment. Assume input power to implanted antenna is -43 dB to investigate patient safety. The other values used to evaluate LM in equations (2)–(4) are mentioned in Table 3 [36, 37].

Three different bitrates were used for transmission data (7, 100 Kbps, and 1 Mbps). As shown in Fig. 11, the antenna can communicate up to 20 m at a bit rate of 7 and 100 Kbps and up to 16 m at a bit rate of 1 Mbps. It is clear that increasing or decreasing the data rate will change the range of data transmission.

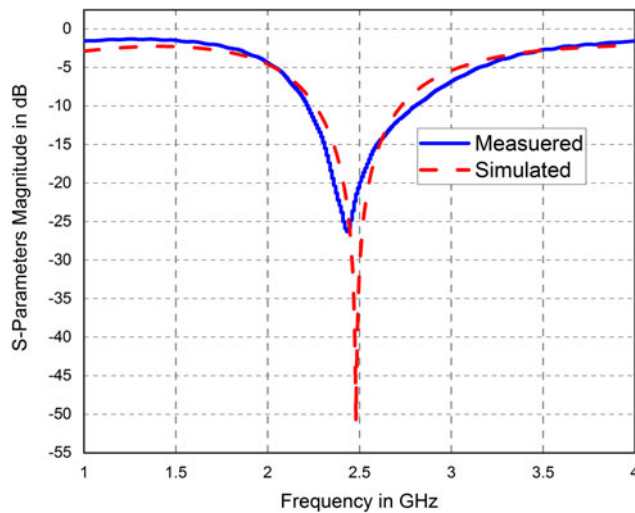


Fig. 13. Simulated and measured reflection coefficient of the presented antenna.

Measurements

In order to validate the designed antenna and confirm the numerical calculations; a prototype of the proposed antenna is fabricated and measured. Due to the difficulty of experimenting with the proposed antenna on human tissues, the performance of the antenna is measured in fresh beef streaky meat with dielectric properties of muscle $\epsilon_r = 53.69$ and fat $\epsilon_r = 3.6$ at frequency 2.45 GHz [38–40]. A piece of meat was selected as closely as possible to that used in the simulations in terms of skin, fat, and muscle. The dimensions of the piece of meat used are approximately $60 \times 60 \times 46 \text{ mm}^3$ and it is implanted at about 2 mm from the skin surface. The prototype of the proposed antenna and the experimental setup images are displayed in Fig. 12.

Comparison between simulated and measured reflection coefficients of the proposed implanted antenna is illustrated in Fig. 13, which they are agreed together quite well. The slight frequency shifting could be caused by the unexpected fabrication tolerance and soldering roughness.

Table 4 illustrates a comparison among the proposed antenna characteristics and the similar literature investigated designs. From Table 4, the merits of the proposed antenna design appear in compact volume and sensitivity of low power as well as lower SAR values.

Conclusions

In this study, an ultra-compact implanted antenna with a size of $5 \times 5 \times 0.26 \text{ mm}^3$ was designed to operate at 2.45 GHz to cover the ISM band. A satisfied gain of -22.5 dBi and a bandwidth of 466 MHz for the proposed antenna is obtained. To determine the main parameters affecting resonant frequency, an intensive parametric study was carried out on CST Microwave Studio. To determine the telemetry range between the ultra-wideband antenna system and the outside base station, the LMs were calculated for different bit rates. The results proved that the antenna could communicate up to 20 m. The SAR has been evaluated and compared with the human health safety standard (IEEE C95.1-1999 and ICNIRP safety regulations). To validate the designed antenna and confirm the calculated numerical results: the proposed antenna was fabricated and measured in a fresh meat box. A

Table 4. Comparison of proposed antenna and prior studies in recent years

Ref.	Frequency (GHz)	Volume (mm^3)	Input power (W)	BW (MHz)	Gain (dBi)	SAR (W/Kg)	Depth (mm)
[35]	2.45	100	1	300	-24.14	217/1 g	N/A
[41]	2.45	99.75	1	520	-26.4	712/1 g	4
[30]	2.6	36.9	-	400	-19.7	0.7 (10 g)	4
[42]	2.45	17.15	1	219	-18.2	305 (1 g)	3
Current work	2.45	6.5	0.5	460	-22.5	40 (10 g)	2

good agreement between simulation and measurement results of the implemented antenna has been achieved. The measured bandwidth is wide enough to cover the whole ISM band with a quite compact volume, making it a good candidate for biomedical applications.

References

- Zada M, Shah IA, Basir A and Yoo H (2021) Ultra-compact implantable antenna with enhanced performance for leadless cardiac pacemaker system. *IEEE Transactions on Antennas and Propagation* **69**, 1152–1157.
- Malik NA, Sant P, Ajmal T and Ur-Rehman M (2021) Implantable antennas for bio-medical applications. *IEEE Journal of Electromagnetics, RF and Microwaves in Medicine and Biology* **5**, 84–96.
- Lin JC and Wang YJ (1987) An implantable microwave antenna for interstitial hyperthermia. *Proceedings of the IEEE* **75**, 1132–1133.
- Ahmed A, Ur-Rehman M and Abbasi QH (2018) Miniature implantable antenna design for blood glucose monitoring, 2018 International Applied Computational Electromagnetics Society Symposium Denver, ACES-Denver 2018, vol. 1, 2–3.
- Rahmat-Samii Y and Kim J (2006) Implanted antennas in medical wireless communications. *Synthesis Lectures on Antennas* **1**, 1–82.
- Manjulatha V and Sri Kavya KC (2016) Implantable antennas for biomedical applications. *Journal of Engineering and Applied Sciences* **11**, 5632–5636.
- Wessels D (2002) Implantable pacemakers and defibrillators: device overview & EMI considerations, IEEE International Symposium on Electromagnetic Compatibility, vol. 2, pp. 911–915.
- Buchegger T, Oßberger G, Reizenzahn A, Hochmair E, Stelzer A and Springer A (2005) Ultra-wideband transceivers for cochlear implants. *EURASIP Journal on Advances in Signal Processing* **2005**, 3069–3075.
- Gosalia K, Lazzi G and Humayun M (2004) Investigation of a microwave data telemetry link for a retinal prosthesis. *IEEE Transactions on Microwave Theory and Techniques* **52**, 1925–1933.
- Shults MC, Rhodes RK, Updike SJ, Gilligan BJ and Reining WN (1994) A telemetry-instrumentation system for monitoring multiple subcutaneous implanted glucose sensors. *IEEE Transactions on Biomedical Engineering* **41**, 937–942.
- Yang X, Fan D, Ren A, Zhao N, Shah SA, Alomainy A, Ur-Rehman M and Abbasi QH (2020) Diagnosis of the hypopnea syndrome in the early stage. *Neural Computing and Applications* **32**, 855–866.
- Zhang Q, Haider D, Wang W, Shah SA, Yang X and Abbasi QH (2018) Chronic obstructive pulmonary disease warning in the approximate ward environment. *Applied Sciences* **8**, 1–16.
- Leelatien P, Ito K, Saito K, Alomainy A, Sharma M and Hao Y (2017) Radio telemetry performance of liver implanted ultra wideband antenna, 2017 11th European Conference on Antennas Propagation, EUCAP 2017, pp. 685–688.
- Scanlon WG, Evans NE and McCreesh ZM (1997) RF performance of a 418-MHz radio telemeter packaged for human vaginal placement. *IEEE Transactions on Biomedical Engineering* **44**, 427–430.
- Savci HS, Sula A, Wang Z, Dogan NS and Arvas E (2005) MICS transceivers: regulatory standards and applications, *Conference Proceedings – IEEE SOUTHEASTCON*, 179–182.
- Geneva S and ITU (2007) Available at <http://itu.int/home>: International Telecommunications Union Radiocommunications (ITU-R), Radio Regulations, SA.1346. Available at www.itu.int/publications.
- 64 Rules Regulations (2010) Medical implant communications service (MICS) federal register. *Federal Register* **75**, 56928–56935.
- Kiourti A, Psathas KA and Nikita KS (2014) Implantable and ingestible medical devices with wireless telemetry functionalities: a review of current status and challenges. *Bioelectromagnetics* **35**, 1–15.
- Kiourti A and Nikita KS (2012) A review of implantable patch antennas for biomedical telemetry: challenges and solutions. *IEEE Antennas and Propagation Magazine* **54**, 210–228.
- Ali WA, Hamad EKI, Bassiuny MA and Hamdallah MZ (2017) Complementary split ring resonator based triple band microstrip antenna for WLAN/WiMAX applications. *Radioengineering* **26**, 78–84.
- Zaki AZA, Abouelnaga TG, Hamad EKI and Elsadek HA (2021) Design of dual-band implanted patch antenna system for bio-medical applications. *Journal of Electrical Engineering* **72**, 240–248.
- Liu XY, Wu ZT, Fan Y and Tentzeris EM (2017) A miniaturized CSRR loaded wide-beamwidth circularly polarized implantable antenna for subcutaneous real-time glucose monitoring. *IEEE Antennas and Wireless Propagation Letters* **16**, 577–580.
- Aboul-Dahab MA, Ghouz HHM and Ahmed Zaki AZ (2016) High gain compact microstrip patch antenna for X-band applications. *International Journal of Antennas* **2**, 47–58.
- Perhirin S and Auffret Y (2013) A low consumption electronic system developed for a 10 km long all-optical extension dedicated to sea floor observatories using power-over-fiber technology and SPI protocol. *Microwave and Optical Technology Letters* **55**, 2562–2568.
- Zhang SWH, Liu L, Li C and Guo Y-X (2013) Miniaturized implantable antenna integrated with split resonator rings for wireless power transfer and data telemetry. *Microwave and Optical Technology Letters* **55**, 2562–2568.
- Faisal F and Yoo H (2019) A miniaturized novel-shape dual-band antenna for implantable applications. *IEEE Transactions on Antennas and Propagation* **67**, 774–783.
- Ibraheem A and Manteghi M (2014) Path loss inside human body using electrically coupled loop antenna at different frequency bands, *IEEE Antennas and Propagation Society AP-S International Symposium*, pp. 977–978.
- Singh G and Kaur J (2021) Skin and brain implantable inset-fed antenna at ISM band for wireless biotelemetry applications. *Microwave and Optical Technology Letters* **63**, 510–515.
- Karacolak T, Hood AZ and Topsakal E (2008) Design of a dual-band implantable antenna and development of skin mimicking gels for continuous glucose monitoring. *Microwave and Optical Technology Letters* **56**, 1001–1008.
- Ketavath KN, Gopi D and Rani SS (2019) In-vitro test of miniaturized CPW-fed implantable conformal patch antenna at ISM band for biomedical applications. *IEEE Access* **7**, 43547–43554.
- Abbasi QH, Ur-Rehman M, Qaraqe K and Alomainy A (2016) *Advances in Body-Centric Wireless Communication: Applications and State-of-the-art*. London, UK: Institution of Engineering and Technology.
- Li R and Xiao S (2014) Compact slotted semi-circular antenna for implantable medical devices. *Electronics Letters* **50**, 1675–1677.
- Das S and Mitra D (2018) A compact wideband flexible implantable slot antenna design with enhanced gain. *IEEE Transactions on Antennas and Propagation* **66**, 4309–4314.
- Sun G, Muneer B, Li Y and Zhu Q (2018) Ultracompact implantable design with integrated wireless power transfer and RF transmission capabilities. *IEEE Transactions on Biomedical Circuits and Systems* **12**, 281–291.
- Bao Z, Guo YX and Mittra R (2018) Conformal capsule antenna with reconfigurable radiation pattern for robust communications. *IEEE Transactions on Antennas and Propagation* **66**, 3354–3365.
- Xia W, Saito K, Takahashi M and Ito K (2009) Performances of an implanted cavity slot antenna embedded in the human arm. *IEEE Transactions on Antennas and Propagation* **57**, 894–899.
- Yousaf M, Mabrouk I, Zada M, Akram A, Amin Y, Nedil M and Yoo H (2021) An ultra-miniaturized antenna with ultra-wide bandwidth characteristics for medical implant systems. *IEEE Access* **9**, 40086–40097.
- Laird ER and Ferguson K (1949) Dielectric properties of some animal tissues at meter and centimeter wave lengths. *The Canadian Journal of Research* **27a**, 218–230.
- Farag KW, Lyng JG, Morgan DJ and Cronin DA (2008) Dielectric and thermophysical properties of different beef meat blends over a temperature range of –18 to +10 °C. *Meat Science* **79**, 740–747.
- Brunton NP, Lyng JG, Zhang L and Jacquier JC (2006) The use of dielectric properties and other physical analyses for assessing protein denaturation in beef biceps femoris muscle during cooking from 5 to 85 °C. *Meat Science* **72**, 236–244.
- Cui W, Liu R, Wang L, Wang M, Zheng H and Li E (2019) Design of wideband implantable antenna for wireless capsule endoscope system. *IEEE Antennas and Wireless Propagation Letters* **18**, 2706–2710.

42. **Shah IA, Zada M and Yoo H** (2019) Design and analysis of a compact-sized multiband spiral-shaped implantable antenna for scalp implantable and leadless pacemaker systems. *IEEE Antennas and Wireless Propagation Letters* 67, 4230–4234.



Ahmed Z. A. Zaki received the B.Sc. degree in electrical engineering (Electronics and Communications) from Modern Academy for Engineering and Technology, Cairo, Egypt in 2008 and the M.Sc. degree from Arab Academy for Science, Technology & Maritime Transport in 2016. From 2010 till now, he is a Teaching Assistant with Modern Academy for Engineering and Technology. He is currently

working toward the Ph.D. degree in designing and optimizing implanted antennas for wireless medical applications at the Faculty of Engineering, Aswan University, Aswan, Egypt. His current research interests include antenna theory, antenna design, medical telemetry, and implantable antennas for bio-medical applications.



Ehab K. I. Hamad received the B.Sc. and M.Sc. degrees in electrical engineering from Assiut University, Egypt in 1994 and 1999, respectively, and the Ph.D. degree in electrical engineering from Magdeburg University, Germany in 2006. From 1996 to 2001, he was a Teaching/Research Assistant with the Faculty of Engineering, South Valley University, Aswan, Egypt. From 2001 to 2006, he was a Research

Assistant with the Chair of Microwave and Communication Engineering, University Magdeburg. From 2010 to 2011, he was with the School of Computing and Engineering, University of Huddersfield, UK as a Postdoctoral Research Assistant. He is currently a Full Professor for antenna engineering with the Faculty of Engineering, Aswan University, Aswan, Egypt. He has authored or coauthored over 60 technical peer-reviewed papers in international journals and conference proceedings. His current research interests include antenna design, MIMO antennas, mm-wave antennas,

metamaterials, RF energy harvesting, and implanted antennas for bio-medical applications.



Tamer Gaber Abouelnaga was born in November 1976. He received his B.Sc. degree (1994–1999, honors degree) in Electronics Engineering from Menofiya University, Egypt, M.Sc. degree (2002–2007), and Ph.D. degree (2007–2012) in Electrical Engineering (Electronics and Communications) from Ain Shams University. He works as a Researcher (2012–2017) and an Associate Professor (2018

till now) in Microstrip Circuits Department, Electronics Research Institute, Egypt. He works as Students Affairs Vice Dean (2018–2019) and Community Service and Environmental Development Vice Dean (2019 till now) – Higher Institute of Engineering and Technology – Kafr Elsheikh City. He had published 36 papers, 25 papers in peer-refereed journals, and 11 papers in international conferences in the area of RFID, horn, MIMO, 5G, and DRA antennas. His current research interests are in hyperthermia breast cancer therapy and human body implanted antennas.



Hala A. Elsadek graduated from Ain Shams University, Egypt, in 1991. She received the Master's degree, Japan, in 1996, and the Ph.D. degree from the University of California, Irvine, USA, in 2002. She is currently a Professor and the Microstrip Department Head and the Technology Development Committee Director of the Electronics Research Institute. Her research interests include RF wireless communications, electromagnetic, and microstrip antenna. She has five books and holds six patents. She is also a single and coauthor in more than 150 articles. She was a recipient of several prizes as Women in Innovation Certificate from the Academy of Scientific Research and Technology, Egypt, 2018; Cambridge International College, Certificate of Recognition, December 2017, the Award for the First Best Researcher in Electronics Research Institutes, in 2019. She acts as a reviewer in many international societies such as the IEEE AP-S and MTT.

metamaterials, RF energy harvesting, and implanted antennas for bio-medical applications.